TASK QUARTERLY 10 No 3, 253–265

APPLICATION OF THE MURNAGHAN MODEL IN ANALYSIS OF NON-LINEAR ELASTIC MATERIAL PROPERTIES OF PVC-COATED FABRIC

ANDRZEJ AMBROZIAK

Department of Structural Mechanics and Bridges Structures,
Faculty of Civil and Environmental Engineering,
Gdansk University of Technology,
Narutowicza 11/12, 80-952 Gdansk, Poland
ambrozan@pg.gda.pl

(Received 22 April 2006)

Abstract: The aim of the present paper is to propose a method of laboratory tests necessary for identification of non-linear elastic properties of the PVC-coated Panama fabric often used for hanging roofs. Two methods of describing the fabric's non-linear behaviour are investigated: piece-wise linear relations between stress and strain are assumed and the Murnaghan model of solid behaviour is applied. The material parameters are specified on the basis of uniaxial constant strain rate tensile tests in the warp and weft directions. Techniques based on the least squares methods are applied in the identification process.

Keywords: non-linear elastic modelling, Murnaghan model, PVC-coated fabric

1. Introduction

Many theoretical laws have been developed for constitutive modelling of PVC-coated fabrics [1, 2]. Various concepts of modelling can be assumed for warp, weft and coating [3], depending on the type of loading and the working conditions. Polymer structures of a fabric may exhibit viscoelastic [4–6], viscoplastic [7] or characteristics [8–11]. The choice of the model is conditioned by the type of coated fabric and the considered kind of loading. In this paper, the PVC-coated Panama fabric is generally assumed to posses non-linear elastic properties. This type of equations can be successfully used in calculations of form finding analysis, initial pre-stressing of a hanging roof, for dynamic analysis of wind action, *etc.*

2. Review of constitutive models of coated fabrics

Numerous constitutive models have been recently developed to describe PVC-coated fabrics. The study of coated fabrics dates back to the early work of Hass [12] and Pierce [13]. These authors presented the crimp theory and described the geometrical and mechanical force models of membrane structures made of woven

fabric. The cross-sectional shape of threads and the crimp pattern were discussed in the crimp theory, while the mechanical properties such as stress and strain were omitted for the sake of mathematical simplicity. The trellis model originally described by Weissenberg [14] and developed by Kilby [15] was historically following model applied to describe the deformations of coated fabrics. In the trellis model, the effect of crimp exchange was neglected. Kawabata *et al.* [16] presented the unit cell model, alternatively referred to as the representative volume element approach. It is one of the methods to obtain material properties for technical materials, knitted or braided fabrics. Wilde [17] studied the problem of dimensioning an unstrained plane membrane to fit the desired surface in the strained state, using the theory of a membrane formed by inextensible cords (*cf.* Rivlin [18]).

Later, Branicki [19] proposed the dense net model, described in detail in the following section. Then, a model based on the micro-mechanical behaviour of a representative unit cell was developed by Nayfeh and Kress [20]. In this model, the global constitutive relationships were consistently derived from the total system strain energy. Various aspects of constitutive modelling for PVC-coated fabrics and novel experimental testing procedures, as well as rheological parameters for viscoelastic materials, were discussed by Argyris *et al.* [5]. Tabiei and Jiang [21] developed the micro-mechanical model describing woven fabrics. Karayaka and Kurath [22] applied the micro-mechanical model in composite finite element analysis based on non-linear stress-strain relationships. Kato *et al.* [23] proposed a formulation of the continuum constitutive equations for fabric membranes. The formulation made use of the fabric lattice model where the structure of fabric membranes was replaced with an equivalent structure composed of truss bars representing the thread net and the coating material. Kuwazuru and Yoshikawa [24] described a pseudo-continuum model for a plain-weave fabric, based on an improved definition of the strain-displacement relationship (see Kuwazuru and Yoshikawa [25] for details). The authors assumed that the fabric's deformations in the pseudo-continuum model are transformed into axial tensile and transverse compressive strains determined individually for the warp and the weft. Xue *et al.* [26] presented a non-orthogonal constitutive model to characterize the woven composites. Relationships between the stresses and strains in the global coordinates were established on the basis of stress and strain analysis in the orthogonal and non-orthogonal coordinates and the rigid body rotation matrices.

In the era of the Internet, it may be worth checking out Arcaro's web page [27], featuring information on design, analysis and interesting references. Arcaro [27] has also developed a simple analytical procedure for cable network structures and a methodology for finding the shape of tension structures.

3. The model

Material composites, including technical woven fabrics, used in membrane roof construction, hanging and pneumatic structures require adequate constitutive modelling describing the material's complex non-linear behaviour.

We usually have two families of threads in a coated fabric (the warp and the weft), which may change their direction in the deformation process. Therefore, the typical isotropic or orthotropic constitutive equations available in every commercial

code cannot be used in its analysis. The plane stress state finite element can be applied to express the fabric's typical properties with a special substructure capable of describing the behaviour of thread families (especially the changing angle between these families during deformation). Such substructure is included in the dense net model proposed in the paper. The dense net model [19, 28] belongs to a group of continuous models, in which three important assumptions are made:

- Stresses T_{11} and T_{22} in given thread families of the warp and the weft depend solely on strains γ_{11} and γ_{22} in the same direction:

$$\begin{aligned} T_{11} &= F_1(\gamma_{11}) \cdot \gamma_{11} \\ T_{22} &= F_2(\gamma_{22}) \cdot \gamma_{22} \end{aligned} \tag{1}$$

  where $F_1(\gamma_{11})$ and $F_2(\gamma_{22})$ specify the tension stiffness of the warp and weft thread families. These parameters are experimentally determined from uniaxial tension tests in the warp and weft directions, respectively. The following matrix form of the substructure's constitutive relations can be obtained for the dense net model:

$$\boldsymbol{T} = \begin{Bmatrix} T_{11} \\ T_{22} \end{Bmatrix} = \begin{bmatrix} F_1(\gamma_{11}) & 0 \\ 0 & F_2(\gamma_{22}) \end{bmatrix} \begin{Bmatrix} \gamma_{11} \\ \gamma_{22} \end{Bmatrix} = \boldsymbol{F}(\boldsymbol{\gamma}) \cdot \boldsymbol{\gamma}. \tag{2}$$

- The material of the warp and the weft is isotropic.
- The warp and weft threads can carry stretching forces only.

An important problem is the choice of range and kind of laboratory tests from which the material parameters are identified. Uniaxial tension tests were chosen here, according to the assumptions of the dense net model. An alternative to this approach would be biaxial tests, but they pose a problem in the selection of the ratio of tensile forces in directions of the weft and warp threads. The ratio's determination in laboratory tests is questionable, because in real structures a different ratio can be observed at each point. There are special constitutive models in which biaxial tensile tests are required to identify the material parameters. For instance, the results of biaxial tests for stress proportions $1:1$, $5:1$ and $1:5$ ($\sigma_{\text{warp}} : \sigma_{\text{weft}}$) are presented in [29] for the fabric model proposed by Day in [30]. Biaxial tensile tests may also be performed for an assumed proportion of strains. For example, biaxial test results for the strain proportion $\varepsilon_{\text{warp}} : \varepsilon_{\text{weft}} = 2$ are given in [31].

In order to derive the elasticity matrix in a local orthogonal system, it is assumed that the warp threads' family, ξ_1, is parallel to the x_1 axis of the local Cartesian coordinate system in the plane stress state finite element and that the weft family, ξ_2, is inclined at angle α (see Figure 1).

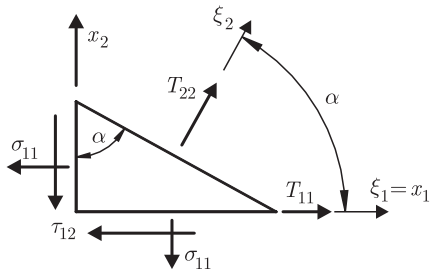

Figure 1. Stress components in the plane stress state

The relation between the plane stress state components, $\boldsymbol{\sigma}$, in local coordinates $\boldsymbol{x}(x_1, x_2)$ of the finite element and the substructure forces in the thread families, $\boldsymbol{T}$ (specific forces), in directions $\boldsymbol{\xi}(\xi_1, \xi_2)$ is defined by transformation matrix $\boldsymbol{C}$:

$$\boldsymbol{\sigma} = \begin{Bmatrix} \sigma_{11} \\ \sigma_{22} \\ \tau_{12} \end{Bmatrix} = \begin{bmatrix} 1 & \cos^2\alpha \\ 0 & \sin^2\alpha \\ 0 & \sin\alpha\cos\alpha \end{bmatrix} \cdot \begin{Bmatrix} T_{11} \\ T_{22} \end{Bmatrix} = \boldsymbol{C} \cdot \boldsymbol{T}. \tag{3}$$

Additionally, the relation between strains γ_{11} and γ_{22} and strains ε_{11}, ε_{22} and ε_{12} in local coordinates $\boldsymbol{x}$, can be specified as follows:

$$\boldsymbol{\gamma} = \begin{Bmatrix} \gamma_{11} \\ \gamma_{22} \end{Bmatrix} = \begin{bmatrix} 1 & 0 & 0 \\ \cos^2\alpha & \sin^2\alpha & \sin\alpha\cos\alpha \end{bmatrix} \cdot \begin{Bmatrix} \varepsilon_{11} \\ \varepsilon_{22} \\ 2\varepsilon_{12} \end{Bmatrix} = \boldsymbol{C}^{\boldsymbol{T}} \cdot \boldsymbol{\varepsilon}. \tag{4}$$

According to Equations (2)–(4), the relation between plane stress state components $\boldsymbol{\sigma}$ and strains $\boldsymbol{\varepsilon}$, can be specified as:

$$\boldsymbol{\sigma} = \boldsymbol{C} \cdot \boldsymbol{T} = \boldsymbol{C} \cdot \boldsymbol{F} \cdot \boldsymbol{\gamma} = \underbrace{\boldsymbol{C} \cdot \boldsymbol{F} \cdot \boldsymbol{C}^{\boldsymbol{T}}}_{\boldsymbol{D}} \cdot \boldsymbol{\varepsilon} = \boldsymbol{D} \cdot \boldsymbol{\varepsilon}, \tag{5}$$

where $\boldsymbol{D}$ defines the elasticity matrix and is expressed as follows:

$$\boldsymbol{D} = \begin{bmatrix} F_1(\gamma_{11}) + F_2(\gamma_{22}) \cdot \cos^4\alpha & F_2(\gamma_{22}) \cdot \sin^2\alpha \cdot \cos^2\alpha & F_2(\gamma_{22}) \cdot \sin\alpha \cdot \cos^3\alpha \\ F_2(\gamma_{22}) \cdot \sin^2\alpha \cdot \cos^2\alpha & F_2(\gamma_{22}) \cdot \sin^4\alpha & F_2(\gamma_{22}) \cdot \sin^3\alpha \cdot \cos\alpha \\ F_2(\gamma_{22}) \cdot \sin\alpha \cdot \cos^3\alpha & F_2(\gamma_{22}) \cdot \sin^3\alpha \cdot \cos\alpha & F_2(\gamma_{22}) \cdot \sin^2\alpha \cdot \cos^2\alpha \end{bmatrix}. \tag{6}$$

The dense net model is capable of expressing the most important properties of fabric materials, which can be determined in uniaxial tension tests in the warp and weft directions only. The model includes the change of the angle between thread families of the warp and the weft during the fabric's deformation. The angle is calculated on the basis of current values of stress components σ_{22} and τ_{12} in the plane stress state from the following relation:

$$\alpha = \arctan\frac{\sigma_{22}}{\tau_{12}}. \tag{7}$$

For a typical coated fabric, the initial value of the angle between thread families is usually $\alpha = \alpha_0 = 90^\circ$.

4. Laboratory tests

The non-linear elastic properties of the PVC-coated Panama fabric were determined on the basis of laboratory tests [32]. The fabric was manufactured from polyester threads of P2/2 weave coated with PVC layers on both sides. A Zwick 147 670 computer-operated strength-testing machine was used in the tests (see Figure 2). Specimens 0.05 m wide and 0.20 m long were cut out in the warp and weft directions. Other important parameters, including the weight of 870 g/m^2 and the initial weave angle of $\alpha_0 = 90^\circ$ were specified by the manufacturer. The results of uniaxial tension tests in the warp and weft threads' directions with constant strain rates of $5 \cdot 10^{-3}$s^{-1}, 10^{-3}s^{-1} and 10^{-4}s^{-1} are given in Figures 3–5 [32]. Various strain rates were used to ascertain the range in which the identified vales could be used. Non-linear elastic properties were determined in the 0.0–0.11 strain range for the

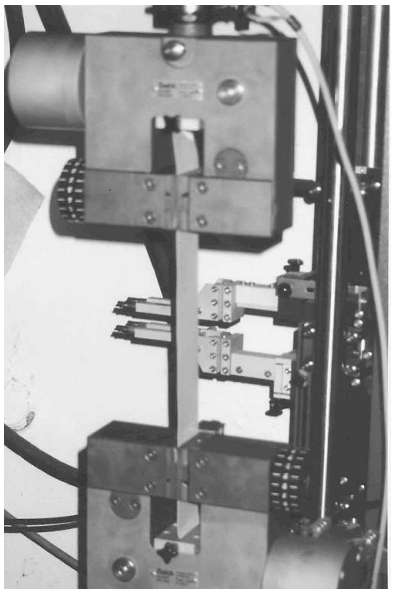

Figure 2. The gripping jaws of the testing machine

warp and the 0.0–0.16 range for the weft. In these strain ranges, the rheological effect can be neglected (see [33] for details).

5. Piecewise linear elastic constitutive description

As shown in Figures 3–5, there are some intervals in which a linear relation between strains and stresses can be assumed; therefore, a piecewise linear description has been proposed. Three coefficients of a straight line for the weft, $F2A$, $F2B$, $F2C$, and the warp, $F1A$, $F1B$, $F1C$ (see Figure 8), specify the longitudinal moduli. The elastic linear model, described below, was used in the admissible strains' range.

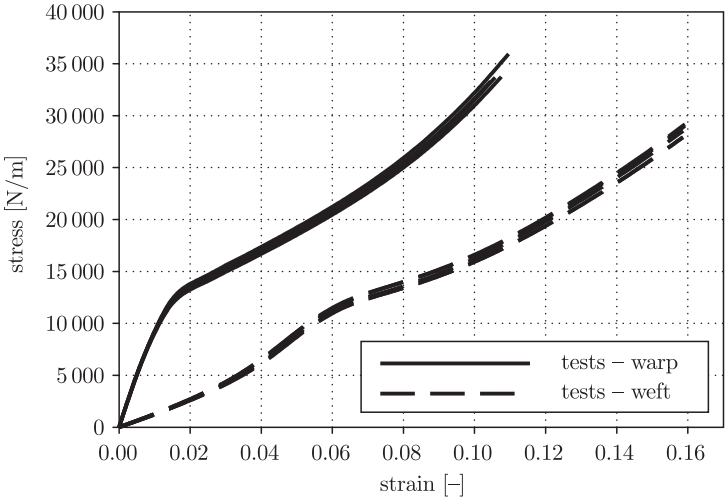

Figure 3. Test results: the strain-stress curve for $\dot{\varepsilon} = 5 \cdot 10^{-3} \mathrm{s}^{-1}$

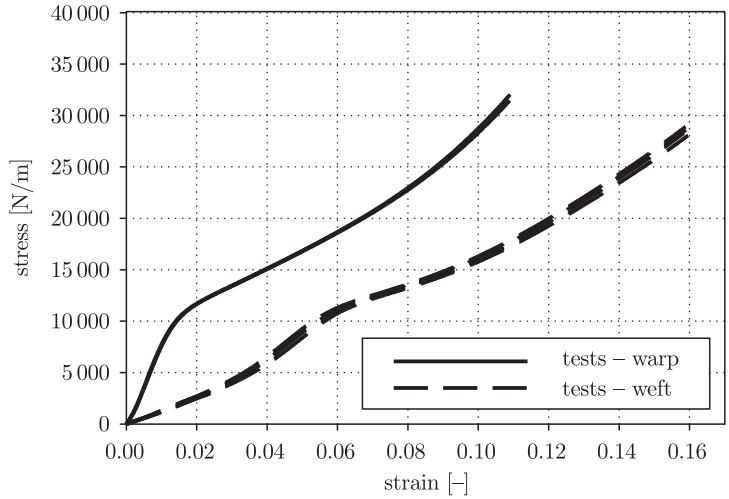

Figure 4. Test results: the strain-stress curve for $\dot{\varepsilon} = 10^{-3}\mathrm{s}^{-1}$

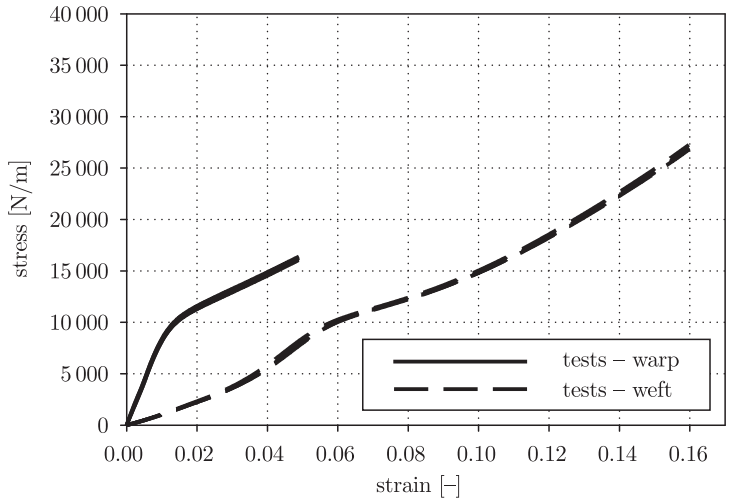

Figure 5. Test results: the strain-stress curve for $\dot{\varepsilon} = 10^{-4}\mathrm{s}^{-1}$

5.1. The model

The relation between stress, $\boldsymbol{S}$, and strain, $\boldsymbol{E}$, tensors in the linear elastic model has the following form (see [34–36] for details):

$$S_{ij} = C_{ijkm}\varepsilon_{km}, \quad \boldsymbol{S} = \boldsymbol{C} \otimes \boldsymbol{E}. \tag{8}$$

The potential energy of a material's adiabatic deformation can be given as:

$$\Phi = \frac{1}{2\boldsymbol{S}} \otimes \boldsymbol{E}. \tag{9}$$

Consequently, the stresses and the elasticity tensor are as follows:

$$S_{ij} = \frac{\partial \Phi}{\partial \varepsilon_{ij}} = \frac{\partial \Phi}{\partial U_{i,j}}, \qquad \boldsymbol{S} = \frac{\partial \Phi}{\partial \boldsymbol{E}}, \tag{10}$$

$$C_{ijkm} = \frac{\partial^2 \Phi}{\partial \varepsilon_{ij} \partial \varepsilon_{km}}, \qquad C = \frac{\partial \boldsymbol{S}}{\partial \boldsymbol{E}} = \frac{\partial}{\partial \boldsymbol{E}} \left(\frac{\partial \Phi}{\partial \boldsymbol{E}} \right). \tag{11}$$

The potential energy accumulated in an isotropic elastic solid can be expressed as:

$$\Phi = \frac{1}{2}(\lambda\delta_{ij}\varepsilon_{kk} + 2\mu\varepsilon_{ij})\varepsilon_{ij} = \frac{1}{2}\lambda(\varepsilon_{mm})^2 + \mu(\varepsilon_{ij})^2. \tag{12}$$

Therefore, Hooke's law for an isotropic material will be:

$$S_{ij} = \lambda\delta_{ij}\varepsilon_{kk} + 2\mu\varepsilon_{ij}, \qquad \boldsymbol{S} = \lambda\,\mathrm{tr}(\boldsymbol{E})\,\boldsymbol{I} + 2\mu\boldsymbol{E}, \tag{13}$$

where λ, μ are the Lamé constants.

5.2. The parameters

In order to describe the uniaxial stress state, we can simplify the energy and stress notations, as strain ε_1 is the principal strain and $\varepsilon_3 = \varepsilon_2$. According to Equations (12) and (13), the components of the stress tensor can be calculated from the following equations:

$$\begin{gathered}\Phi = \frac{1}{2}\lambda(\varepsilon_{mm})^2 + \mu(\varepsilon_{ij})^2 \Rightarrow S_{ij} = \frac{\partial\Phi}{\partial\varepsilon_{ij}} = \lambda\delta_{ij}\varepsilon_{kk} + 2\mu\varepsilon_{ij}, \\ S_{11} = \lambda(\varepsilon_1 + 2\varepsilon_2) + 2\mu\varepsilon_1 \quad S_{22} = S_{33} = \lambda(\varepsilon_1 + 2\varepsilon_2) + 2\mu\varepsilon_2.\end{gathered} \tag{14}$$

It should be noted that stress component S_{11} is a function of the unknown strain ε_2. This strain can be determined from the assumption of the uniaxial stress state, $S_{22} = S_{33} = 0$. Subject to this assumption, it is possible to calculate ε_2 directly:

$$\lambda(\varepsilon_1 + 2\varepsilon_2) + 2\mu\varepsilon_2 = 0 \quad \Rightarrow \quad \varepsilon_2 = -\frac{\lambda\varepsilon_1}{2\lambda + 2\mu}. \tag{15}$$

Lamé constants of $\lambda = 4\,989\,616\,745\,\mathrm{N/m}$, $\mu = 318\,642\,\mathrm{N/m}$ can be assumed on the basis of laboratory tests (*e.g.* warp_31, see Figure 6). The longitudinal elasticity modulus, F, can be determined from known values of the Lamé constants, as follows:

$$F = \frac{\mu(3\lambda + 2\mu)}{\lambda + \mu} = \frac{318\,642(3\cdot 4\,989\,616\,745 + 2\cdot 318\,642)}{4\,989\,616\,745 + 318\,642} = 955\,907\,\mathrm{N/m} \tag{16}$$

It is also possible to obtain the longitudinal modulus, F, directly from laboratory tests:

$$S_{11} = F\cdot\varepsilon_1. \tag{17}$$

The value of $F = 955\,907\,\mathrm{N/m}$ can be obtained from a linear approximation (*e.g.* warp_31, see Figure 7). This example of elastic parameter determination has confirmed the assumed identification procedure and will be extended in the following section to the Murnaghan model.

The final results of are given in Table 1 and Figure 8.

Table 1. Non-linear elastic properties of coated fabric Panama [33]

	[kN/m]	[—]
warp	$F1A = 904$	$\varepsilon_{P1} = 0.0119$
	$F1B = 176$	$\varepsilon_{P2} = 0.093$
	$F1C = 471$	$\varepsilon_{P3} = 0.110$
weft	$F2A = 187$	$\varepsilon_{P1} = 0.039$
	$F2B = 146$	$\varepsilon_{P2} = 0.1495$
	$F2C = 340$	$\varepsilon_{P3} = 0.160$

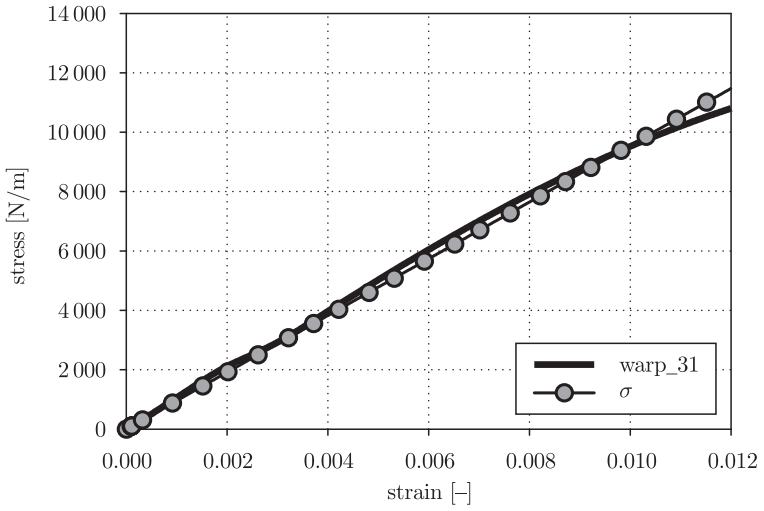

Figure 6. Identification of parameters λ and μ; $\boldsymbol{\sigma} = \lambda \mathrm{tr}(\boldsymbol{\varepsilon})\boldsymbol{I} + 2\mu\boldsymbol{\varepsilon}$

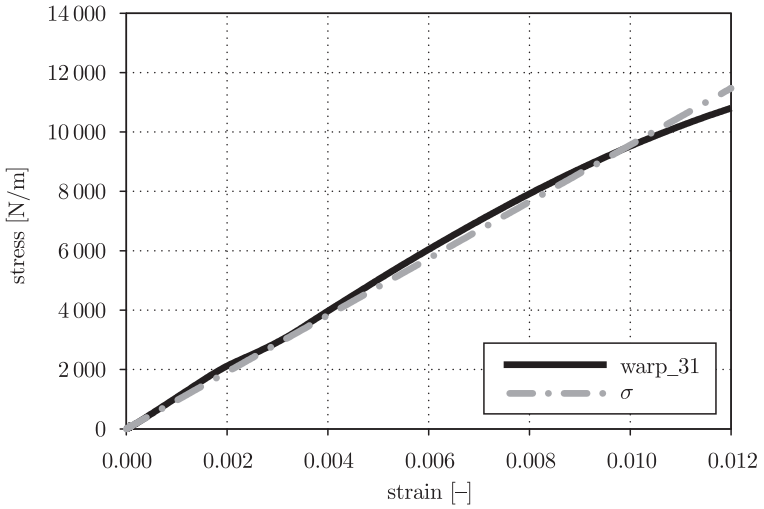

Figure 7. Identification of parameter F; $\boldsymbol{\sigma} = F\boldsymbol{\varepsilon}$

6. The Murnaghan model-based description of threads' behaviour

6.1. The model

The material model of the Murnaghan solid has been chosen for this analysis. In the Murnaghan solid model, potential energy is given by the following equation (*cf.* Murnaghan [37], Guz [38]):

$$\Phi = \frac{1}{2}\lambda (E_{mm})^2 + \mu (E_{ij})^2 + \frac{1}{3}AE_{ij}E_{im}E_{jm} + B(E_{ij})^2 E_{mm} + \frac{1}{3}C(E_{mm})^3, \qquad (18)$$

where λ, μ are the Lamé constants and A, B, C are Murnaghan constants, while E_{ij} are components of the Lagrange-Green strain tensor. It should be noted that the Murnaghan proposal of energy approximation is not the only one found in the

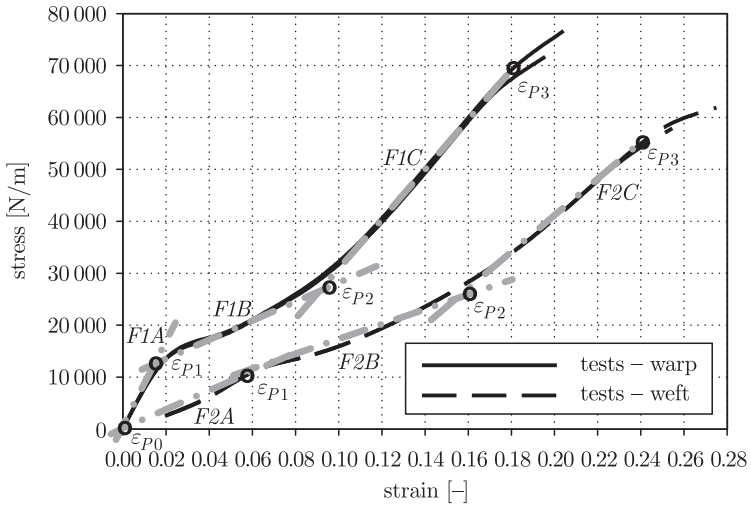

Figure 8. Graphical interpretation of the F parameters

literature (*e.g.* the Mooney potential was proposed for incompressible media, the Blaz-Ko potential for a rubber-like material, *etc.*; *cf.* Lurie [39]).

The invariants of the Lagrange-Green strain tensor can be specified from the principal strain components as follows:

$$\begin{aligned} I_{\boldsymbol{E}} &= \operatorname{tr}(\boldsymbol{E}) = \varepsilon_1+\varepsilon_2+\varepsilon_3, \\ II_{\boldsymbol{E}} &= \frac{1}{2}\left(\operatorname{tr}\left(\boldsymbol{E}^2\right)-\left(\operatorname{tr}(\boldsymbol{E})\right)^2\right) = \varepsilon_1\varepsilon_2+\varepsilon_1\varepsilon_3+\varepsilon_2\varepsilon_3, \\ III_{\boldsymbol{E}} &= \det(\boldsymbol{E}) = \varepsilon_1\varepsilon_2\varepsilon_3. \end{aligned} \tag{19}$$

With the Lagrange-Green strain tensor invariants Equation (19), the potential energy can be written in the following form (see [40]):

$$\Phi = \frac{\lambda+2\mu}{2}\left(I_{\boldsymbol{E}}\right)^2 - 2\mu II_{\boldsymbol{E}} + \frac{l+2m}{3}\left(I_{\boldsymbol{E}}\right)^3 - 2m\left(I_{\boldsymbol{E}}\right) II_{\boldsymbol{E}} + n III_{\boldsymbol{E}}, \tag{20}$$

where λ, μ are the Lamé constants (the same as in the piecewise model) and l, m, n are the Murnaghan constants. The second Piola-Kirchhoff stress $\boldsymbol{S}$ is derived as the gradient of energy Φ with respect to $\boldsymbol{E}$:

$$\boldsymbol{S} = \left(\frac{\lambda-2\mu}{3} I_{\boldsymbol{E}} - (2m-n)\, II_{\boldsymbol{E}} + l\left(I_{\boldsymbol{E}}\right)^2\right)\boldsymbol{I} + \left(2\mu + (2m-n)\, I_{\boldsymbol{E}}\right)\boldsymbol{E} + n\boldsymbol{E}^2. \tag{21}$$

In a particular case of the uniaxial stress state, strains ε_2 and ε_3 are equal. The Lagrange-Green strain tensor invariants have the following form:

$$\begin{aligned} I_{\boldsymbol{E}} &= \operatorname{tr}(\boldsymbol{E}) = \varepsilon_1+2\varepsilon_2, \\ II_{\boldsymbol{E}} &= \frac{1}{2}\left(\operatorname{tr}\left(\boldsymbol{E}^2\right)-\left(\operatorname{tr}(\boldsymbol{E})\right)^2\right) = 2\varepsilon_1\varepsilon_2+\varepsilon_2^2, \\ III_{\boldsymbol{E}} &= \det(\boldsymbol{E}) = \varepsilon_1\varepsilon_2^2. \end{aligned} \tag{22}$$

Then, the potential energy can be determined from the following equation:

$$\begin{aligned} \Phi = {} & \frac{\lambda+2\mu}{2}\left(\varepsilon_1+2\varepsilon_2\right)^2 - 2\mu\left(2\varepsilon_1\varepsilon_2+\varepsilon_2^2\right) + \frac{l+2m}{3}\left(\varepsilon_1+2\varepsilon_2\right)^3 + \\ & - 2\, m\left(2\varepsilon_1^2\varepsilon_2+\varepsilon_1\varepsilon_2^2+4\varepsilon_1\varepsilon_2^2+2\varepsilon_2^3\right) + n\left(\varepsilon_1\varepsilon_2^2\right). \end{aligned} \tag{23}$$

Finally, the stress components are:

$$\begin{aligned} S_{11} = \frac{\partial \Phi}{\partial \varepsilon_1} &= (\lambda+2\mu)(2\varepsilon_1+4\varepsilon_2) - 2\mu 2\varepsilon_2 + \\ &(l+2m)(\varepsilon_1+2\varepsilon_2)^2 - 2\ m\left(4\varepsilon_1\varepsilon_2+5\varepsilon_2^2\right)+n\varepsilon_2^2 \\ &= \varepsilon_1^2(l+2\ m)+\varepsilon_1(4\varepsilon_2 l+\lambda+2\mu)+\varepsilon_2(\varepsilon_2(4l-2m+n)+2\lambda) \end{aligned} \tag{24}$$

and

$$\begin{aligned} S_{22} = S_{33} = \frac{\partial \Phi}{\partial \varepsilon_2} &= (\lambda+2\mu)(4\varepsilon_1+8\varepsilon_2) - 2\mu(2\varepsilon_1+2\varepsilon_2)+2(l+2m) \\ &(\varepsilon_1+2\varepsilon_2)^2 - 2\ m\left(2\varepsilon_1^2+2\varepsilon_1\varepsilon_2+8\varepsilon_1\varepsilon_2+6\varepsilon_2^2\right)+2n\varepsilon_1\varepsilon_2 = \\ &= 2\left(\varepsilon_1^2 l+\varepsilon_1(\varepsilon_2(4l-2m+n)+\lambda)+2\varepsilon_2^2(2l+m)+2\varepsilon_2(\lambda+\mu)\right). \end{aligned} \tag{25}$$

As in the previous section, it is necessary to solve the $S_{22}=0$ equation, from which the unknown component of strain ε_2 can be determined, but the solution is complex, as Equation (25) is a second-order polynomial function of ε_2.

6.2. The parameters

The least squares' regression was applied to determine the material parameters for the Murnaghan model. The Marquardt-Levensberg algorithm [41] was used to find the coefficients of the independent variables that offer the best fit between the equation and the experimental data. On the basis of this numerical algorithm, coefficients λ, μ, l, m, n were specified for the warp (see Table 2) and the weft (see Table 3) for each laboratory test. The final results of material parameters' identification (mean values of coefficients λ, μ, l, m, n) are given in Table 4.

Table 2. Murnaghan coefficients – warp

$\dot{\varepsilon}$ [s^{-1}]	Test name	λ [N/m]	μ [N/m]	l [N/m]	m [N/m]	n [N/m]
$5\cdot10^{-3}$	warp_28.dat	217 359	−169 386	490 705	7 656 987	569 059
	warp_29.dat	220 888	−172 635	487 578	8 063 491	584 134
	warp_30.dat	213 300	−166 544	359 732	7 344 501	646 027
	warp_31.dat	223 891	−175 007	389 555	7 865 657	655 358
10^{-3}	warp_39.dat	161 423	−122 861	366 898	5 125 476	479 067
	warp_40.dat	170 763	−130 627	471 656	5 869 332	443 733
10^{-4}	warp_21.dat	185 276	−143 879	35 248	5 926 780	877 349
	warp_22.dat	174 453	−134 854	66 376	5 460 992	821 003
	warp_23.dat	185 475	−143 951	164 318	6216 755	786 354

6.3. Numerical simulation

In order to verify the obtained results, numerical simulations of uniaxial tension tests were performed for the established mean values of the Murnaghan coefficients. The results of these calculations are shown in Figures 9–11. Good agreement of the stress-strain relations obtained from numerical simulations and laboratory tests has been observed.

Table 3. Murnaghan coefficients – weft

$\dot{\varepsilon}$ [s^{-1}]	Test name	λ [N/m]	μ [N/m]	l [N/m]	m [N/m]	n [N/m]
$5 \cdot 10^{-3}$	weft_10.dat	50289	−25899	467252	1841328	−51889
	weft_11.dat	49836	−25447	461703	1814737	−49034
	weft_12.dat	50289	−25900	467263	1841288	−51836
	weft_13.dat	50289	−25900	467263	1841290	−51836
	weft_14.dat	50289	−25900	467263	1841289	−51839
10^{-3}	weft_05.dat	50289	−25900	467263	1841290	−51831
	weft_06.dat	49293	−24931	456730	1800611	−35776
	weft_07.dat	49475	−25248	457295	1808588	−37596
	weft_08.dat	47852	−23794	445091	1738241	−37879
10^{-4}	weft_09.dat	45382	−22470	450760	1746863	−48903
	weft_15.dat	44185	−21728	429388	1674444	−30684
	weft_16.dat	44826	−22477	416207	1648747	−18314
	weft_17.dat	45851	−22904	455993	1772193	−51090

Table 4. Murnaghan coefficients for PVC-coated Panama fabric

	$\bar{\lambda}$ [kN/m]	$\bar{\mu}$ [kN/m]	$\bar{l}$ [kN/m]	$\bar{m}$ [kN/m]	$\bar{n}$ [kN/m]
warp	188.9	−146.2	313.3	6366.0	634.4
weft	48.2	−24.4	453.6	1781.2	−43.1

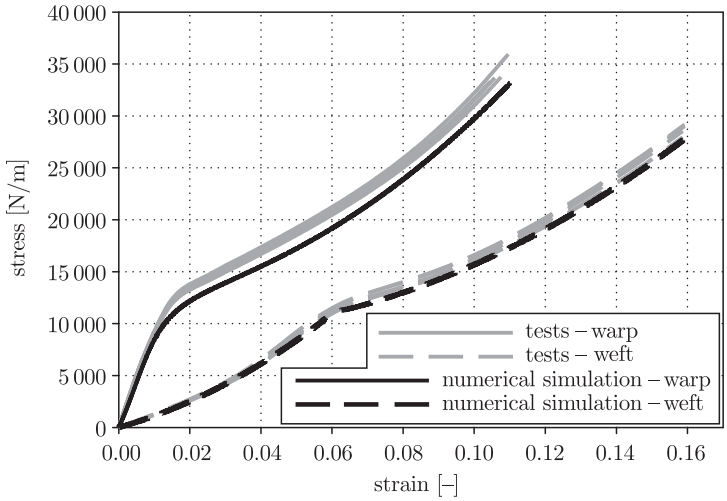

Figure 9. Calculation results: comparison with laboratory tests ($\dot{\varepsilon} = 5 \cdot 10^{-3} s^{-1}$)

7. Conclusions

The non-linear elastic Murnaghan model has been successfully applied on the basis of uniaxial tension tests to describe the behaviour of a PVC-coated Panama fabric. The model can be applied in a wide range of engineering problems. The material

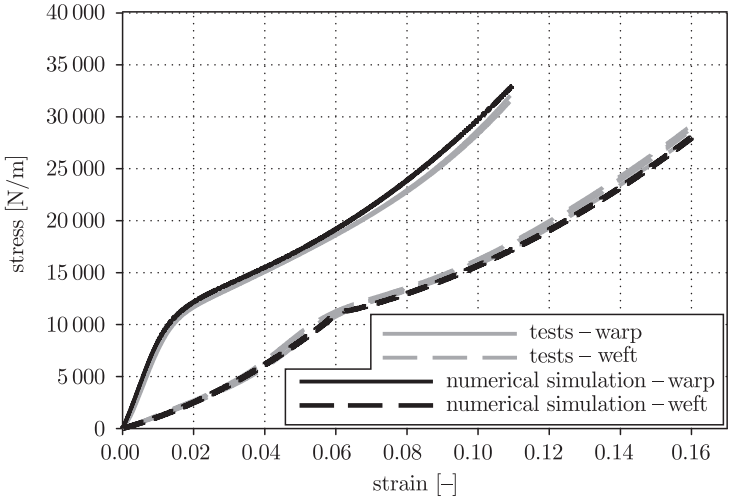

Figure 10. Calculation results: comparison with laboratory tests ($\dot{\varepsilon} = 10^{-3}\,\mathrm{s}^{-1}$)

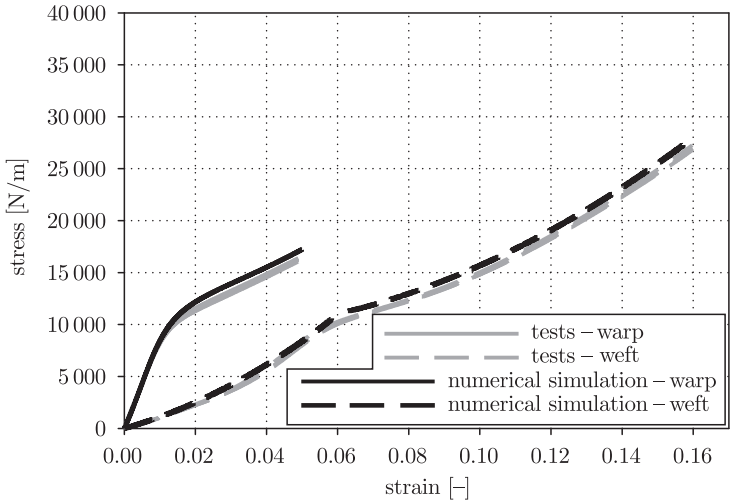

Figure 11. Calculation results: comparison with laboratory tests ($\dot{\varepsilon} = 10^{-4}\,\mathrm{s}^{-1}$)

parameters determined above can be used directly in FEM to analyze structures made of PVC-coated fabrics, where geometric non-linearity is accompanied by the physical non-linearity of the fabric's material.

References

[1] Ambroziak A and Kłosowski P 2003 *Workshop on Advanced Mechanics of Urban Structures*, Sopot, Poland, pp. 145–148

[2] Ambroziak A and Kłosowski P 2005 *Lightweight Structures in Civil Engineering* (Micro-Publ. Obrębski J B Ed.), Warsaw, pp. 99–102

[3] Ambroziak A and Kłosowski P 2005 *Textile Composites and Inflatable Structures II* (Oñate E and Kröplin B Eds), CIMNE, Barcelona, pp. 131–138

[4] Argyris J, Doltsinis J S and Silva V D 1991 *Comp. Meth. Appl. Mech. Eng.* **88** 135

[5] Argyris J, Doltsinis J S and Silva V D 1992 *Comp. Meth. Appl. Mech. Eng.* **98** 159

[6] Kłosowski P and Komar W 2004 *Proc. of the 8th Int. Conf. Modern Building Materials, Struct. and Techniques*, Vilnus, Lithuania, pp. 790–795
[7] Kłosowski P, Zagubień A and Woznica K 2004 *Arch. Appl. Mech.* **73** 661
[8] Bejan L and Poterasu V F 1999 *Com. Methods Appl. Mech. Eng.* **179** 53
[9] Jensen J J 1972 *Proc. 1971 IASS Pacyfic Symposium*, Arch. Inst. of Japan., Tokyo, pp. 176–183
[10] Peng X and Cao J 2002 *Composites Part B: Engineering* **33** 45
[11] Wizmur M 1969 *Engineering Transactions*, Gdansk University of Technology **1** 17 (in Polish)
[12] Haas R 1918 *National Advisory Committee for Aeronautics Report* **16** 155
[13] Peirce F T 1937 *J. Textile Institute* **28** T45
[14] Weissenberg K 1949 *J. Textile Institute* **40** T89
[15] Kilby W F 1963 *J. Textile Institute* **54** T9
[16] Kawabata S, Niwa M and Kawai H 1973 *J. Textile Institute* **64** 21; **64** 47
[17] Wilde P 1966 *Arch. Appl. Mech.* **18** 463
[18] Rivlin R S 1959 *Arch. Rat. Mech.* **2** 83
[19] Branicki C 1969 *Some static problems of hanging nets*, PhD thesis, Gdansk University of Technology (in Polish)
[20] Nayfeh A H and Kress G R 1997 *Composites Part B: Engineering* **28** 627
[21] Tabiei A and Jiang Y 1999 *Int. J. Solids Struct.* **36** 2757
[22] Karayaka M and Kurath P 1994 *J. Eng. Mater. Technol.* **116** 222
[23] Kato S, Yoshino T and Minami H 1999 *Eng. Struct.* **21** 691
[24] Kuwazuru O, Yoshikawa N 2003 *Int. Conf. on Textile Composites and Inflatable Struct.*, Barcelona, Spain, pp. 335–340
[25] Kuwazuru O, Yoshikawa N 2001 *The 33rd Int. SAMPE Tech. Conf. „SAMPLE"*, Seattle, USA, pp. 564–573
[26] Xue P, Peng X and Cao J 2003 *Composites Part A: Applied Science and Manufacturing* **34** 183
[27] Arcaro V F http://www.arcaro.org/tension/index.htm
[28] Branicki C and Kłosowski P 1983 *Arch. Civil Eng.* **29** 189 (in Polish)
[29] Bridgens B N and Gosling P D 2004 *Computer and Struct.* **82** 1913
[30] Day A S 1986 *IASS Symposium Proc.: Shells, Membranes and Space Frames*, Elsevier, Osaka-Amsterdam, pp. 17–24
[31] Buet-Gautier K and Boisse P 2001 *Experimental Mech.* **41** (3) 260
[32] Zagubień A 2002 *Laboratory Tests and Identification of Inelastic Properties of Panama Coated Fabric*, PhD Thesis, Koszalin University of Technology (in Polish)
[33] Ambroziak A 2005 *TASK Quart.* **9** (2) 167
[34] Fung Y C 1965 *Foundations of Solid Mechanics*, Prentice-Hall, Englewood Cliffs, New Jersey
[35] Green A E and Zerna W 1960 *Theoretical Elasticity*, Clarendon Press, Oxford
[36] Hartman F 1985 *The Mathematical Foundation of Structural Mechanics*, Springer-Verlag, Berlin–Heidelberg–New York–Tokyo
[37] Murnaghan F D 1951 *Finite Deformation of an Elastic Solid*, John Wiley, New York
[38] Guz A N 1999 *Fundamentals of the Three-dimensional Theory of Stability of Deformable Bodies*, Sprinter-Verlag, Berlin
[39] Lurie A I 1990 *Nonlinear Theory of Elasticity*, Elsevier
[40] Lurie A I 1970 *Theory of Elasticity*, Nauka, Moscow (in Russian)
[41] Marquardt D W 1963 *J. Soc. Ind. Appl. Math.* **11** 431